Synthesis of Germanium Nanoclusters with Irreversibly Attached Functional Groups: Acetals, Alcohols, Esters, and Polymers

Robin S. Tanke,*,† Susan M. Kauzlarich,*,‡ Timothy E. Patten,*,‡ Katherine A. Pettigrew,‡ Drew L. Murphy,§ Mark E. Thompson,§ and Howard W. H. Lee||

Department of Chemistry, University of Wisconsin-Stevens Point, Stevens Point, Wisconsin 54481, Department of Chemistry, University of California, Davis, One Shields Avenue, Davis, California 95616-5295, Department of Chemistry, University of Southern California, Los Angeles, California 90089-1062, and UltraDots Inc., 48611 Warm Springs Boulevard, Fremont, California 94539

Received December 6, 2002. Revised Manuscript Received February 13, 2003

Germanium nanoclusters of average diameter 4 nm were prepared with covalently bound termination groups. Chloride-terminated nanoclusters were reacted with a Grignard reagent to form acetal-containing surface-terminated nanoclusters. Treatment with acid yielded hydroxyl-containing surface-terminated nanoclusters, and treatment with an acid bromide and base yielded an ester-containing surface-terminated nanocluster. Atom transfer radical polymerization (ATRP) was used to graft polymer chains from the surfaces of the nanoparticles to yield hybrid nanostructures. Changes of the termination group in the nanoclusters did not alter the photophysics of the original nanoclusters, a result that is consistent with a stable nanocluster surface. The nanoclusters were characterized by HRTEM (high-resolution transmission electron microscopy), NMR, FTIR, UV−vis, and fluorescence spectroscopy.

Introduction

The size-dependent luminescent and nonlinear optical properties of semiconductor nanoclusters make them attractive candidates for a variety of technological applications.[1,2] Monodisperse, well-characterized samples of II−VI semiconductor nanoclusters can be readily prepared.[3−8] Consequently, many groups have demonstrated that CdS and CdSe nanoclusters[6−11] are useful in a number of technologies including light-emitting diodes (LEDs), photodiodes, photovoltaic solar cells, gas sensors, and fluorescent labeling.

Nanocluster surfaces must be stabilized because the nanoclusters are unstable relative to bulk material. This is generally accomplished by covering the surface of the nanocluster with a monolayer of organic material that will be referred to as the termination group. This organic monolayer is important not only for the stabilization of the nanocluster but also for many of the applications of these nanoclusters.[12] For example, luminescent probes have been prepared[7] by attaching oligonucleotides to CdSe/ZnS nanoclusters via chemical manipulation of a thiol termination group. Photocatalysts for the generation of hydrogen from 2-propanol have been prepared[13] by immobilizing CdS/ZnS on thiol-modified polystyrene. The use of phosphine oxides, amines, and thiols as the termination groups for II−IV nanoclusters is common; however, in many cases these termination groups can be displaced.[14,15] Furthermore, Aldana and co-workers[16] have shown that the thiols attached to CdSe undergo photocatalytic oxidation to disulfides, which eventually leads to nanocluster aggregation. The loss of the initial termination group through displacement and photocatalytic oxidation of thiol termination groups make II−VI nanoclusters unsatisfactory for some applications.

* Authors to whom correspondence should be addressed.
† University of Wisconsin-Stevens Point.
‡ University of California, Davis.
§ University of Southern California.
|| UltraDots Inc.

(1) Heath, J. R. *Acc. Chem. Res.* **1999**, *32*, 387.
(2) Alivisatos, A. P. *Science* **1996**, *271*, 933.
(3) Weller, H. *Angew. Chem., Int. Ed. Engl.* **1993**, *32*, 41.
(4) Murray, C. B.; Norris, D. J.; Bawendi, M. G. *J. Am. Chem. Soc.* **1993**, *115*, 8706.
(5) Wang, Y.; Herron, N. *J. Phys. Chem.* **1991**, *95*, 525.
(6) Chan, W. C. W.; Nie, S. *Science* **1998**, *281*, 2016.
(7) Pathak, S.; Choi, S.-K.; Arnheim, N.; Thompson, M. E. *J. Am. Chem. Soc.* **2001**, *123*, 4103.
(8) Godovsky, D. Y. *Adv. Polym. Sci.* **2000**, *153*, 163.
(9) Bruchez, M.; Moronne, M.; Gin, P.; Weiss, S.; Alivisatos, A. P. *Science* **1998**, *281*, 2013.
(10) Mattoussi, H.; Mauro, J. M.; Goldman, E. R.; Anderson, G. P.; Sundar, V. C.; Mikulec, F. V.; Bawendi, M. G. *J. Am. Chem. Soc.* **2000**, *122*, 12142.
(11) Willard, D. M.; Carillo, L. L.; Jung, J.; Orden, A. V. *Nano Lett.* **2001**, *1*, 581.
(12) Sieval, A. B.; Linke, R.; Zuilhof, H.; Sudholter, E. J. R. *Adv. Mater.* **2000**, *12*, 1457.
(13) Hirai, T.; Saito, T.; Komasawa, I. *J. Phys. Chem. B* **2001**, *105*, 9711.
(14) Gerion, D.; Pinaud, F.; Williams, S. C.; Parak, W. J.; Zanchet, D.; Weiss, S.; Alivisatos, A. P. *J. Phys. Chem. B* **2001**, *105*, 8861.
(15) Peng, X. G.; Schlamp, M. C.; Kadavanich, A. V.; Alivisatos, A. P. *J. Am. Chem. Soc.* **1997**, *119*, 7019.
(16) Aldana, J.; Wang, Y. A.; Peng, X. *J. Am. Chem. Soc.* **2001**, *123*, 8844.

10.1021/cm021778h CCC: $25.00 © 2003 American Chemical Society
Published on Web 03/28/2003

Scheme 1. Synthetic Scheme for Preparing Surface-Functionalized Germanium Nanoclusters

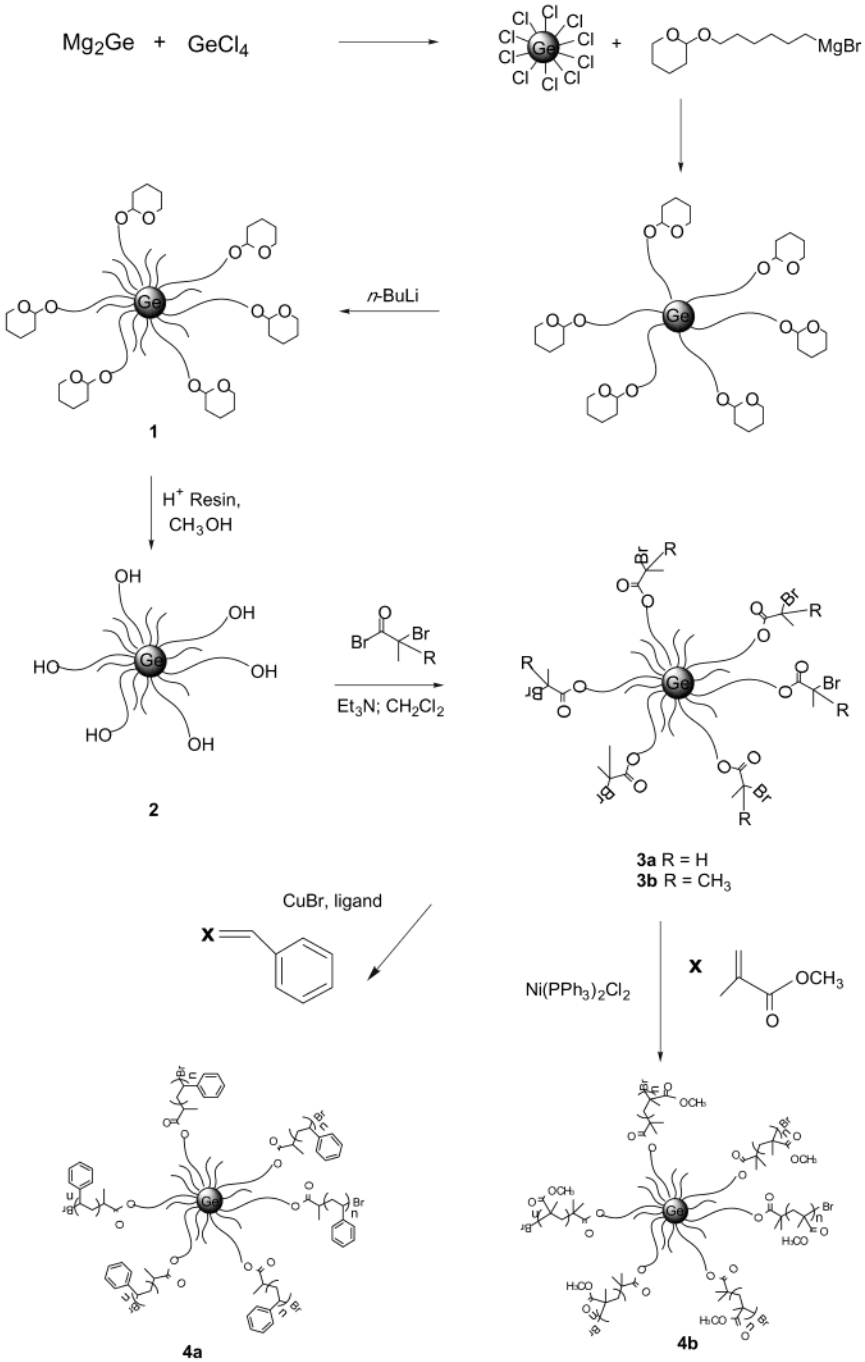

Germanium and other group IV nanoclusters are gaining attention and reported applications of group IV nanoclusters are quite promising.[17−42] Many of the reported syntheses[27] for group IV nanoclusters offer little control of the termination group and occur at temperatures >500 °C. However, solution syntheses of silicon[32−35,39−42] and germanium[31,36−38] nanoclusters with alkyl termination groups have been reported. Furthermore, nanocluster formation occurs under moderate conditions and results in the formation of covalent bonds between carbon and the group IV nanocluster surface. However, because alkyl groups are not easily chemically manipulated, the alkyl-terminated group IV nanoclusters are limited in their applications. This paper describes the preparation of germanium nanoparticles of average diameter 4 ± 2 nm with termination groups containing functionality and how this functionality can be readily manipulated using established synthetic methodology. The first preparation of germanium nanoclusters terminated with organic groups containing acetals, alcohols, esters, and polymer chains (Scheme 1) is reported.

(17) Ding, Z. F.; Quinn, B. M.; Haram, S. K.; Pell, L. E.; Korgel, B. A.; Bard, A. J. *Science* **2002**, *296*, 1293.
(18) Watanabe, A.; Unno, M.; Hojo, F.; Miwa, T. *Chem. Lett.* **2001**, 1092.
(19) Watanabe, A.; Sato, T.; Matsuda, M. *Jpn. J. Appl. Phys. 1* **2001**, *40*, 6457.
(20) Watanabe, A.; Unno, M.; Hojo, F.; Miwa, T. *J. Mater. Sci. Lett.* **2001**, *20*, 491.
(21) Holmes, J. D.; Ziegler, K. J.; Doty, R. C.; Pell, L. E.; Johnston, K. P.; Korgel, B. A. *J. Am. Chem. Soc.* **2001**, *123*, 3743.
(22) Nayfeh, M. H.; Akcakir, O.; Belomoin, G.; Barry, N.; Therrien, J.; Gratton, E. *Appl. Phys. Lett.* **2000**, *77*, 4086.

Experimental Section

Materials. Mg_2Ge was prepared from magnesium flake purchased from Aesar and germanium purchased from Aldrich.[43] 1-Bromo-6-tetrahydropyranyl-oxyhexane[44,45] was prepared from 1-bromo-6-hexanol (Aldrich), 2,3-dihydropyran (Aldrich), and pyridinium *p*-toluenesulfonate, or it was purchased from Sigma. 2-Methoxyethyl ether (Aldrich, anhydrous, 99.5%) was distilled twice from Na−K alloy under argon. THF was distilled from Na/benzophenone. Dichloromethane was treated by stirring over sulfuric acid, washing with water, then $NaHCO_3$ (aq), drying over $MgSO_4$, and distilled from CaH_2 prior to use. Methyl methacrylate and triethylamine were distilled from calcium hydride. Styrene and xylene (Fisher) were distilled prior to use. HPLC-grade water (Fisher), HPLC-grade methanol (Fisher), HPLC-grade hexane (Aldrich), spectrophotometric-grade chloroform (Fisher), and HPLC-grade tetrahydrofuran (Acros) were used as received. Unless specified otherwise, all other reagents were purchased from commercial sources and used as received.

Characterization. ^{13}C {^1H} and ^1H NMR spectra were recorded on a Varian Mercury 300 NMR spectrometer. Solid-state NMR spectra were obtained with a Chemagnetics CMX-400 spectrometer using a standard Chemagnetics cross-polarization MAS probe assembly configured for rotors having an outer diameter of 7.5 mm. The samples were packed into zirconium oxide rotors having O-ring sealed PTFE plugs. No significant background signal was observed for ^{13}C, for this configuration. Sample rotation rates varied from 3.2 to 6.0 kHz, depending on the experiment and the positions of principal absorption peaks. Typically, 1000−2000 acquisitions were averaged per spectrum. Chemical shifts were referenced to the proton or carbon signal of chloroform. FTIR spectra were obtained with a Mattson Galaxy Series FTIR 3000. UV−vis spectra were obtained with a HP 8452A diode array spectrophotometer. Photoluminescence spectra were recorded on a Perkin-Elmer LS 50B luminescence spectrophotometer. Quantum efficiency measurements were carried out at room temperature in $CHCl_3$ on a Photon Technology International fluorimeter. Chloroform solutions of Coumarin 47 were used as a reference.[46] Powder X-ray diffraction data were collected with an INEL CPS 120 diffractometer utilizing Cu $K\alpha_1$ radiation. The electron microscope was a Phillips CM200 operating at 200-keV accelerating voltage at the National Center for Electron Microscopy (NCEM). HRTEM samples of germanium nanoclusters with butyl and 6-tetrahydropyranyloxy hexyl termination, **1**, with butyl and with butyl and 6-hydroxyl termination, **2**, were prepared by dipping a carbon-coated 300-mesh copper grid into a sonicated chloroform solution of the nanoclusters. Electron-dispersive X-ray (EDX) spectroscopy was also obtained on these samples. Polymerization kinetics were monitored using gas chromatography. Number-averaged molecular weights (M_n), weight-averaged molecular weights (M_w), and molecular weight distributions (M_w/M_n) were determined using gel-permeation chromatography (GPC) in THF at 30 °C and a flow rate of 1 mL min^{-1}. Three Polymer Standards Services columns (100 Å, 1000 Å, and linear) were connected to a Thermoseparations Products P-100 isocratic pump, autosampler, column oven, and Knauer refractive index detector. The system was calibrated using polystyrene standards from Polymer Standard Services; M_p = 400−1000000; $M_w/M_n < 1.10$.

Germanium Nanoclusters with Butyl and (6-Tetrahydropyranyloxy)hexyl Termination Groups (1). A 500-mL three-neck round-bottom flask was equipped with a reflux condenser, a vacuum adapter, stir bar, and glass stoppers and was brought into a drybox. Magnesium germanide (426 mg, 3.56 mmol) was added. Out of the drybox, 250 mL of 2-methoxyethyl ether was transferred via cannula onto the magnesium germanide. The mixture was brought to reflux under argon. After refluxing overnight, the mixture was cooled to ambient temperature, germanium tetrachloride (1.40 mL, 12.4 mmol) was added, and the mixture was heated to reflux. The gray solid disappeared, giving a colorless solution. The mixture was then allowed to stir at reflux for 24 h and then was cooled to ambient temperature. 2-Methoxy ethyl ether and excess $GeCl_4$ were removed in vacuo, and then fresh 2-methoxy ethyl ether (∼200 mL) was added. Meanwhile, a 250-mL three-neck round-bottom flask equipped with a reflux condenser, stir bar, addition funnel, and vacuum adapter was brought into the drybox and charged with 680 mg (30.0 mmol) of magnesium. THF (30 mL) was added to the magnesium. In a separate flask 1-bromo-6-tetrahydropyranyl-oxyhexane (3.11 g, 12.4 mmol) and 20 mL of THF were mixed and then added to the addition funnel. A small amount of the THF/alkyl bromide solution was added to the flask, and the flask was warmed gently. 1,2-Dibromoethane (0.5 mL) was added to start the reaction. Once the reaction started, the THF/alkyl bromide solution was added dropwise over a period of 15 min. After addition was complete, the mixture was stirred at 40 °C for 4 h. The Grignard reagent was then added via cannula to the germanium particles in 2-methoxy ethyl ether, and the mixture was stirred at ambient temperature for 16 h. Then, 2.2 mL of butyl lithium (1.6 M solution in hexane) was added at ambient temperature, and the mixture was stirred for 6 h. The solvent was removed in vacuo. The residue was extracted with 150 mL of HPLC-grade water and 100 mL of HPLC-grade hexane. The hexane layer was extracted with 2 × 100 mL of HPLC-grade water. The initial water layer was back-extracted with 50 mL of HPLC-grade hexane. The hexane layers were combined and washed with 50 mL of HPLC-grade water. The hexane was removed via rotary evaporation, and the residue was dissolved in spectrophotometric-grade chloroform. The chloroform was removed in vacuo, and high boiling organics were removed by distillation at 130 °C and 50 mTorr. The residue, 1.16 g, was used directly in the next reaction without further purification. Minor peaks in the ^1H NMR spectra were

(23) Nayfeh, M. H.; Barry, N.; Therrien, J.; Akcakir, O.; Gratton, E.; Belomoin, G. *Appl. Phys. Lett.* **2001**, *78*, 1131.
(24) Nayfeh, M. H.; Rao, S.; Barry, N.; Therrien, J.; Belomoin, G.; Smith, A.; Chaieb, S. *Appl. Phys. Lett.* **2002**, *80*, 121.
(25) Therrien, J.; Belomoin, G.; Nayfeh, M. *Appl. Phys. Lett.* **2000**, *77*, 1668.
(26) Delgado, G. R.; Lee, H. W. H.; Parak, W. J.; Fulks, R. T.; Parsons, G. N.; Slobodin, D. E.; Yuzuriha, T. H. *Mater. Res. Soc. Flat Panel Display Mater. III Symp.* **1997**, 263.
(27) King, W. D.; Boxall, D. L.; Lukehart, C. M. *J. Cluster Sci.* **1997**, *8*, 267.
(28) Wilcoxon, J. P.; Provencio, P. P.; Samara, G. A. *Phys. Rev. B* **2001**, *6403*, 5417.
(29) Carpenter, J. P.; Lukehard, C. M.; Henderson, D. O.; Mu, R.; Jone, B. D.; Glosser, R.; Stock, S. R.; Wittig, J. E.; Zhu, J. G. *Chem. Mater.* **1996**, *8*, 1268.
(30) Kornowski, A.; Giersig, M.; Vogel, R.; Chemseddine, A.; Weller, H. *Adv. Mater.* **1993**, *5*, 634.
(31) Heath, J. R.; Shiang, J. J.; Alivisatos, A. P. *J. Chem. Phys.* **1994**, *101*, 1607.
(32) Bley, R. A.; Kauzlarich, S. M. *J. Am. Chem. Soc.* **1996**, *118*, 12461.
(33) Kauzlarich, S. M. *Abstr. Pap. Am. Chem. Soc.* **2000**, *219*, U821.
(34) Lee, H. W. H. T.; Peter, A.; Delgado, G. R.; Kauzlarich, S. M.; Yang, C.-S.; Taylor, B. R. *Crit. Rev. Opt. Sci. Technol.* **2000**, *CR77*, 147.
(35) Liu, Q.; Kauzlarich, S. M. *Mater. Sci. Eng., B* **2002**, *B96*, 72.
(36) Taylor, B. R.; Kauzlarich, S. M.; Lee, H. W. H.; Delgado, G. R. *Chem. Mater.* **1998**, *10*, 22.
(37) Taylor, B. R.; Kauzlarich, S. M.; Delgado, G. R.; Lee, H. W. H. *Chem. Mater.* **1999**, *11*, 2493.
(38) Taylor, B. R.; Fox, G. A.; Hope-Weeks, L. J.; Maxwell, R. S.; Kauzlarich, S. M.; Lee, H. W. H. *Mater. Sci. Eng., B* **2002**, *96*, 90.
(39) Yang, C.-S.; Bley, R. A.; Kauzlarich, S. M.; Lee, H. W. H.; Delgado, G. R. *J. Am. Chem. Soc.* **1999**, *121*, 5191.
(40) Yang, C. S.; Kauzlarich, S. M.; Wang, Y. C. *Chem. Mater.* **1999**, *11*, 3666.
(41) Yang, C. S.; Liu, Q.; Kauzlarich, S. M.; Phillips, B. *Chem. Mater.* **2000**, *12*, 983.
(42) Yang, C. S.; Kauzlarich, S. M.; Wang, Y. C.; Lee, H. W. H. *J. Cluster Sci.* **2000**, *11*, 423.
(43) Klemm, W.; Westlingning, Z. *Z. Anorg. Chem.* **1941**, 265.
(44) Miyashita, N.; Yoshikoshi, A.; Grieco, P. A. *J. Org. Chem.* **1977**, *42*, 3772.
(45) Collie, L.; Denness, J. E.; Parker, D.; Ocarroll, F.; Tachon, C. *J. Chem. Soc., Perkin Trans. 2* **1993**, 1747.
(46) Bos, F. *Appl. Opt.* **1981**, *20*, 3553.

observed. Major peaks were as follows. ^{1}H NMR (300 MHz, $CDCl_3$): 4.55 (pseudo triplet, O−CH−O), 3.85 (m), 3.73 (m), 3.47 (m), 3.38 (m), 1.79 (m), 1.67 (m), 1.4−1.6 (broad), 1.4−1.2 (broad), 0.88 (broad pseudotriplet). ^{13}C NMR (75 MHz, $CDCl_3$): 98.7, 67.7, 67.6, 62.2, 33.5−32.4 (multiple peaks), 30.8, 29.7−29.5 (multiple peaks), 26.3−25.9 (multiple peaks), 25.6, 19.7, 13.7(CH_3). IR (neat): 2940 (s), 2856 (s), 1465 (m), 1351 (m), 1261 (m) 1199 (m), 1138 (s), 1078 (s), 1033 (s), 870 (m), 816 (m) cm^{-1}. In the distillate 2-(hexyloxy)tetrahydropyran (CAS registry number 1927-63-5) and an unidentified primary olefin are the major byproducts by ^{1}H and ^{13}C NMR spectra interpretation.

Germanium Nanoclusters with Butyl and 6-Hydroxyhexyl Termination Groups (2). To **1** (1.06 g) in a 100-mL round-bottom flask equipped with a stir bar, 50 mL of HPLC-grade methanol was added along with 0.92 g of Dowex 50 × 2-100 ion-exchange resin. The mixture was stirred at ambient temperature for 5.5 h. The mixture was filtered through Celite to remove the resin. The methanol was removed via rotary evaporation. The residue was washed with HPLC-grade hexanes, and the residue was taken up in spectrophotometric-grade chloroform. The chloroform was removed in vacuo to yield 866.7 mg of waxy material. ^{1}H NMR (300 MHz, $CDCl_3$): 3.61 (t, OCH_2), 1.53 (m), 1.34−1.24 (bm), 0.86 (m, CH_3). ^{13}C NMR (75 MHz, $CDCl_3$): 63.1, 62.9, 32.8−32.6 (multiple peaks), 29.7, −29.4 (multiple peaks), 25.8, 25.6, 13.8. IR (neat): 3342 (m), 2923(s), 2850 (s), 1479 (m), 1384 (m), 1059 (m), 1041 (m), 991 (w), 870 (w), 818 (w), 688 (w), 615 (w) cm^{-1}.

Germanium Nanoclusters with Butyl and 6-(2-Bromopropionyloxy)hexyl Termination Groups (3a). To **2** (649.5 mg) in a 100-mL round-bottom flask equipped with a stir bar, 50 mL of freshly distilled CH_2Cl_2, 0.300 mL (2.13 mmol) of triethylamine and 0.45 mL (4.30 mmol) of 2-bromopropionyl bromide were added. The solution was stirred at ambient temperature for 17.5 h. The solution was transferred to a separatory funnel, and 50 mL of distilled CH_2Cl_2 was added. The solution was washed with 3 × 100 mL of saturated sodium bicarbonate, 2 × 50 mL of 2 M HCl (aq), and then 50 mL of HPLC-grade water. The CH_2Cl_2 was removed in vacuo, and volatile organics were removed by distillation (120 °C, 50 mTorr) to yield 747.7 mg of **3a**. ^{1}H NMR (300 MHz, $CDCl_3$): 4.34 (pseudoquartet, CHBr), 4.12 (m, CH_2O), 1.78 (d, CHBrCH_3), 1.63 (m), 1.4−1.24 (bm), 1.1 (m), 0.88 (m). ^{13}C NMR (75 MHz, $CDCl_3$): 170.0 (C═O), 66.0, 65.83, 40.2 (CHBr), 32.4−31.7 (multiple peaks), 29.5, 29.4, 29.2, 28.3, 28.2, 28.1, 25.7, 25.6, 21.7, 13.7. IR (neat) 2927 (s), 2856 (m), 1743 (s), 1446 (m), 1336 (m), 1224(s), 1159 (s), 1060 (m), 802 (w), 679 (w) cm^{-1}.

Germanium Nanoclusters with Butyl and 6-(2-Bromoisobutyloxy)hexyl Termination Groups (3b). The nanoclusters **3b** were prepared as above from 2-bromoisobutyl bromide. ^{1}H NMR (300 MHz, $CDCl_3$): 4.15 (t, CH2O), 1.92 (s, C(CH3)2), 1.65 (broad), 1.39 (broad), 1.2 (broad), 0.90 (broad). ^{13}C NMR (75 MHz, $CDCl_3$): 171.5 (C═O), 66.1, 66.0, 56.0 ($C(CH_3)_2Br$), 32.1−33.8 (multiple peak), 30.8 ($C(CH_3)_2Br$), 29.5, 29.2, 28.4, 28.2, 24.6−25.8 (multiple peaks), 23.9, 20.3, 18.8, 13.8. IR (neat): 2928 (s), 2856 (m), 1735 (s), 1464 (m), 1370 (m), 1277 (s), 1164 (s), 1110 (s), 869 (w), 299 (w) cm^{-1}.

Polymerization of Styrene Using 3a as the Initiator (4a). A 25-mL Schlenk flask was charged with a stir bar, CuBr (63.7 mg, 0.444 mmol), 4,4′-di(5-nonyl)-2,2′-bipyridine (365.0 mg, 0.893 mmol), 2.0 mL of *p*-xylene, 5.0 mL (43.6 mmol) of styrene, and 114.9 mg of **3**. The mixture was put through three freeze−pump−thaw cycles and placed in a constant-temperature bath at 110 °C, and 0.5 mL aliquots were taken periodically. The aliquots were dissolved in 5.0 mL of THF, filtered through Al_2O_3, and precipitated in methanol. The solid (**4a**) was filtered, and portions were dissolved in THF for GPC analysis.

Removal of Polystyrene Chains by Transesterification. In a 100-mL round-bottom flask, **4a** (133.2 mg), 10 mL of potassium hydroxide in methanol (5 g/100 mL), toluene (15 mL), and THF (15 mL) were added. The solution was heated at reflux for 16 h. The polystyrene was isolated by precipitation from methanol and filtration. Samples were analyzed by GPC.

Polymerization of Methyl Methacrylate Using 3b as the Initiator (4b). A 25-mL Schlenk flask was charged with a stir bar, $NiBr_2(PPh_3)_2$ (150 mg, 0.20 mmol), 1.1 mL of *p*-xylene, 4.0 mL (37.3 mmol) of methyl methacrylate, and 80.8 mg of **3b**. The mixture was put through three freeze−pump−thaw cycles and placed in a constant-temperature bath at 100 °C. Aliquots of 0.5 mL were taken periodically. The aliquots were dissolved in 5.0 mL of THF, reacted with Dowex ion-exchange resin,[47] and filtered. The poly(methyl methacrylate) (PMMA) coated nanoclusters were then precipitated in methanol. The solid (**4b**) was filtered, and portions were dissolved in THF for GPC analysis.

Reaction of Germanium Tetrachloride with 6-Tetrahydropyranyl Hexyl Magnesium Bromide and Butyl Lithium. 1-Bromo-6-tetrahydropyranyloxy hexane (1.185 g, 4.47 mmol) and magnesium were used to prepare the tetrahydropyranyloxy hexyl magnesium bromide in THF. The magnesium bromide solution was transferred via cannula to a solution of germanium tetrachloride (0.10 mL, 0.89 mmol) in dry 2-methoxy ethyl ether (30 mL) and a white precipitate immediately formed. The mixture was stirred at ambient temperature for 16 h and the butyl lithium (0.7 mL of 1.6 M in hexanes (Aldrich)) was added. The solvent was removed in vacuo and HPLC-grade hexanes and water were added to separate salts from organic material. The hexane was removed in vacuo and the crude reaction mixture was distilled at 130 °C and 0.5 Torr to remove volatile organics; 0.412 g of residue was isolated. ^{1}H NMR ($CDCl_3$): 4.53 (t), 3.81 (m), 3.67 (m), 3.41 (m), 3.33 (m), 1.77 (m), 1.66 (m), 1.59 (m), 1.28 (m), 0.83 (t), 0.7 (bm), 0.63 (bm). ^{13}C NMR ($CDCl_3$): 98.9, 67.7, 62.4, 33.8, 33.7, 31.0, 30.0, 29.8, 29.7, 27.7, 26.9, 26.5, 26.1, 25.8, 19.9, 14.3, 14.0, 13.0, 12.7. IR (neat, NaCl plates): 2931 (s), 2870 (s), 1466 (m), 1344 (m), 1200 (m), 1119 (s), 1079 (s), 1033 (s), 987 (m), 870 (m), 815 (w) cm^{-1}. A chloroform solution of this material did not photoluminesce. In the distillate (0.098 g) 2-(hexyloxy)tetrahydropyran (CAS registry number 1927-63-5) and an unidentified primary olefin are the major byproducts by ^{1}H and ^{13}C NMR spectra interpretation.

Results and Discussion

Preparation of Acetal-Terminated Nanoclusters. Germanium nanoclusters of average diameter 4 ± 2 nm were prepared with acetal termination groups (**1**) using a modification of the solution synthesis described by Taylor and co-workers.[36−38] Magnesium germanide was reacted with germanium tetrachloride in refluxing 2-methoxy ethyl ether. After the solution was cooled to room temperature and excess germanium tetrachloride was removed, freshly prepared (6-tetrahydropyranyloxy)hexyl magnesium bromide was added and allowed to react at ambient temperature for 16 h and then *n*-butyl lithium was added. The resulting nanoclusters, **1**, containing both butyl and (6-tetrahydropyranyloxy)-hexyl termination groups, were soluble in hexane and chloroform. Nanoclusters were prepared with mixed termination groups because attempts to prepare the nanoparticle with only the (6-tetrahydropyranyloxy)-hexyl group lead to products with unstable photoluminescence. Over a period of time, the nanoclusters, terminated only with the (6-tetrahydropyranyloxy)hexyl group, lost their photoluminescence and a white precipitate formed. The precipitate was dried, heated at 150 °C overnight, and determined to be GeO_2 by X-ray powder diffraction. The instability of these nanoparticles is attributed to incomplete termination of the surface, resulting in oxidation of the Ge nanocluster. In contrast, the nanoclusters employing mixed termination groups

(47) Matyjaszewski, K.; Pintauer, T.; Gaynor, S. *Macromolecules* **2000**, *33*, 1476.

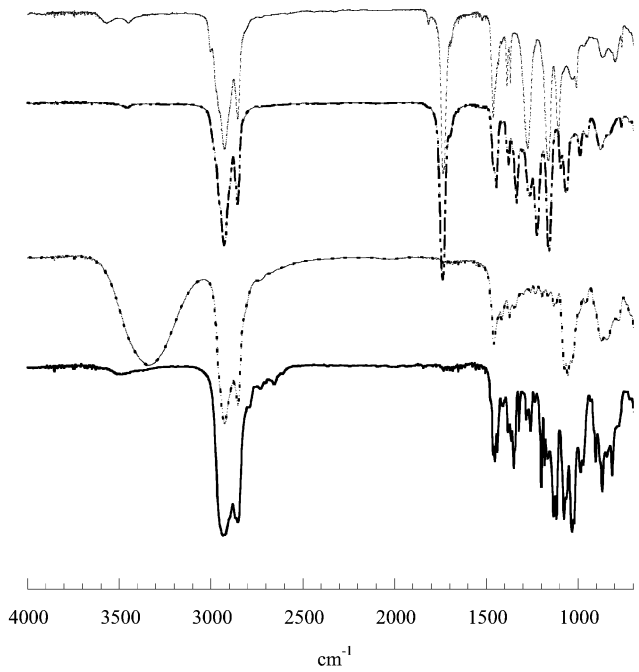

Figure 1. IR spectra of germanium nanoclusters starting from the bottom nanoclusters-**1** (acetal-containing surface termination), -**2** (alcohol-containing surface termination), -**3a** (α-bromopropanoate ester-containing surface termination), and -**3b** (α-bromoisobutanoate ester-containing surface termination).

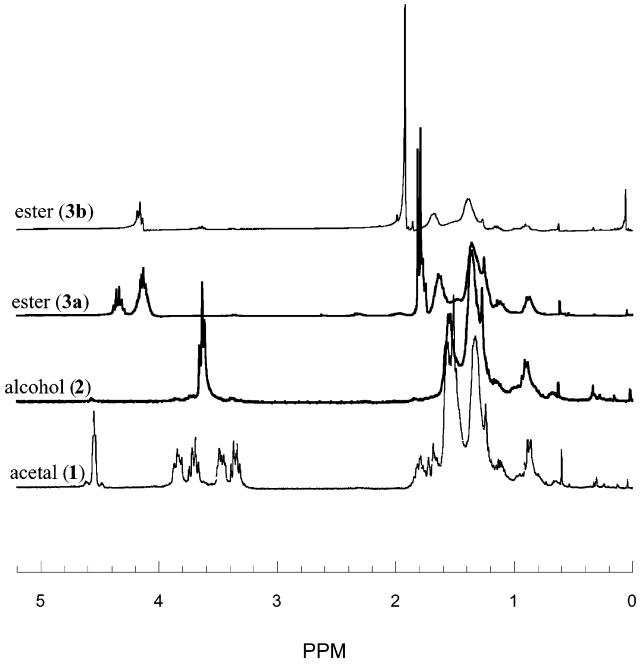

Figure 2. ^{1}H NMR spectra of germanium nanoclusters-**1** (acetal-containing surface termination), -**2** (alcohol-containing surface termination), -**3a** (α-bromopropanoate ester-containing surface termination), and -**3b** (α-bromoisobutanoate ester-containing surface termination).

maintained their photoluminescence for over 11 months. By integration of the ^{1}H NMR spectrum of **1**, the ratio of acetal termination groups to butyl groups is about 3:1. Inorganic salts were separated from nanoclusters **1** by aqueous extraction and organics were removed by distillation.

Preparation of Hydroxy-Terminated Nanoclusters. To prepare germanium nanoclusters with mixed butyl and 6-hydroxyhexyl termination groups (**2**), the THP protecting group was removed with methanol and Dowex 50 × 2-100 ion-exchange resin as a proton source. A solid-phase acid catalyst was chosen because the hydroxyl-terminated nanoclusters were expected to be water-soluble. The resin afforded a means by which the acid could be separated by filtration rather than aqueous extraction. The IR spectra of the acetal **1**- and the alcohol **2**-terminated nanoclusters are shown in Figure 1. The IR spectrum of **2** shows a new O−H stretch at 3342 cm^{-1}, indicating the removal of the THP group. Unlike **1**, the nanoclusters, **2**, are waxy solids and are insoluble in hexane and slightly soluble in water.

Preparation of Ester-Terminated Nanoclusters. The hydroxy-terminated particles, **2**, represent a good starting material for a variety of synthetic transformations, as hydroxyl groups can be transformed via simple reactions into halides, esters, ethers, silyl ethers, aldehydes, and ketones.[48] The esters were prepared by reacting **2** with triethylamine and 2-bromopropionyl bromide or 2-bromoisobutyl bromide to yield esterified germanium nanoclusters (**3a** and **3b**, respectively) The IR spectra (Figure 1) of **3a** and **3b** showed C═O stretches at 1743 and 1735 cm^{-1}, respectively, indicating the presence of the ester group. The termination with an α-bromoester is important because α-bromoesters are initiators for the controlled/"living" radical polymerizations.[49,50] The nanoclusters, **3a** and **3b**, were soluble in a variety of solvents including chloroform, dichloromethane, styrene, and methyl methacrylate.

NMR Spectra of Nanoclusters 1−3. Sharp resonances corresponding to acetal, alcohol, and ester functionalities are observed in the ^{1}H and ^{13}C{^{1}H} NMR spectra (Figures 2 and 3) of germanium nanoclusters **1**−**3**. This is expected as they are far removed from the nanocluster core, and since our synthesis produces a range of sizes, the solution NMR is dominated by the smallest nanoclusters, probably about 1−2 nm in diameter. This is further supported by the photoluminescent spectra, which reflects the average size of the nanoclusters, described below. In addition, ^{13}C{^{1}H} MAS solid-state NMR provides the same spectra, so we believe that these NMR are representative of the entire sample. When gold nanoclusters are stabilized with alkane thiols, full-width at half-maximum intensity (fwhm) of the carbons closest to the sulfur headgroup is larger than the fwhm of the carbons further from the sulfur headgroup in the ^{13}C{^{1}H} NMR spectra.[51−54] This

(48) Carey, F. A.; Sundberg, R. J. *Advanced Organic Chemistry*, 4th ed.; Kluwer Academic/Plenum Pub.: New York, 2000.

(49) Patten, T. E.; Matyjaszewski, K. *Adv. Mater.* **1998**, *10*, 901.
(50) Patten, T. E.; Matyjaszewski, K. *Acc. Chem. Res.* **1999**, *32*, 895.
(51) Kohlmann, O.; Steinmetz, W. E.; Mao, X. A.; Wuelfing, W. P.; Templeton, A. C.; Murray, R. W.; Johnson, C. S. *J. Phys. Chem. B* **2001**, *105*, 8801.
(52) Terrill, R. H.; Postlethwaite, T. A.; Chen, C. H.; Poon, C. D.; Terzis, A.; Chen, A. D.; Hutchison, J. E.; Clark, M. R.; Wignall, G.; Londono, J. D.; Superfine, R.; Falvo, M.; Johnson, C. S.; Samulski, E. T.; Murray, R. W. *J. Am. Chem. Soc.* **1995**, *117*, 12537.
(53) Badia, A.; Gao, W.; Singh, S.; Demers, L.; Cuccia, L.; Reven, L. *Langmuir* **1996**, *12*, 1262.
(54) Hostetler, M. J.; Wingate, J. E.; Zhong, C. J.; Harris, J. E.; Vachet, R. W.; Clark, M. R.; Londono, J. D.; Green, S. J.; Stokes, J. J.; Wignall, G. D.; Glish, G. L.; Porter, M. D.; Evans, N. D.; Murray, R. W. *Langmuir* **1998**, *14*, 17.

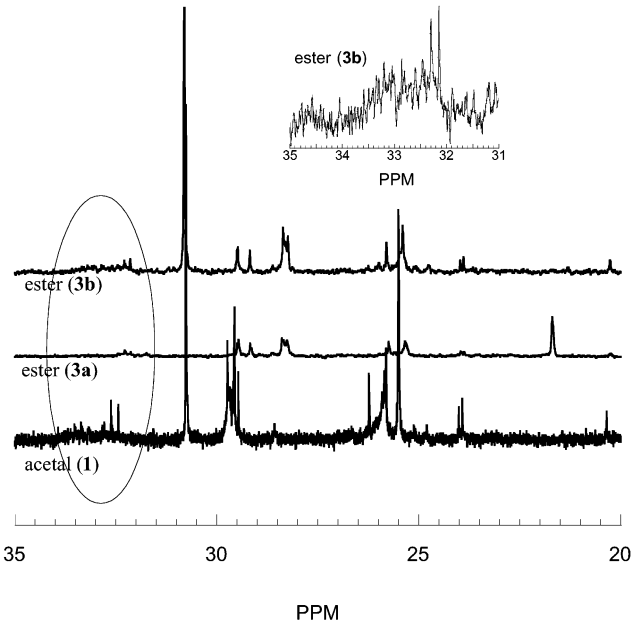

Figure 3. ^{13}C $\{^1H\}$ NMR spectra of germanium nanoclusters-**1** (acetal-containing surface termination), -**3a** (α-bromopropanoate ester-containing surface termination), and -**3b** (α-bromoisobutanoate ester-containing surface termination).

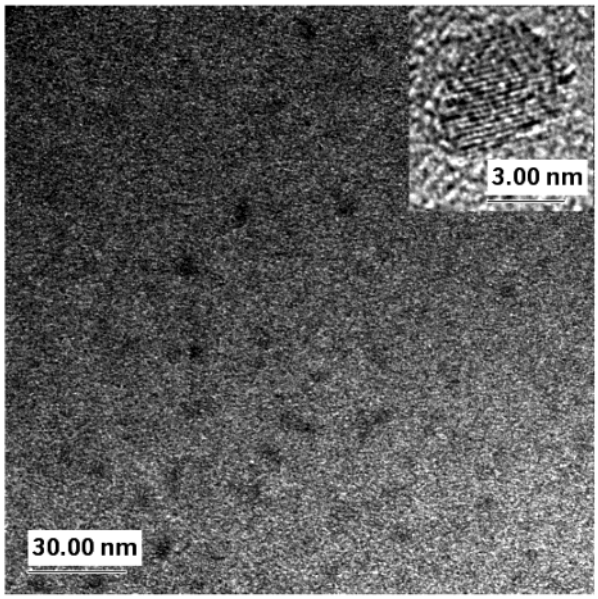

Figure 4. HRTEM image of nanoclusters **1**. The insert shows the lattice fringes of the {220} crystal plane.

increase in fwhm for protons attached to carbons closest to the sulfur headgroup is also observed in the ^1H NMR spectra. Hostetler et al.[54] have established that the line broadening increases with nanocluster size and several factors are believed to contribute to the observed line broadening. Factors include fast spin relaxation due to dipolar interactions caused by the solidlike nature of the methylene groups near the gold core, different binding sites for the thiol groups on the nanocluster surface, and increased spin−spin relaxation time for groups closest to the nanocluster core due to nanocluster tumbling. The resonances in the ^1H and $^{13}C\{^1H\}$ NMR spectra allow the monitoring of the functional group. For nanocluster **1**, the acetal proton resonance at 4.55 ppm and the acetal carbon resonance at 98.7 ppm supported the presence of the THP group. The $^{13}C\{^1H\}$ and ^1H NMR spectra of nanoclusters **2** were also consistent with removal of the THP group: noted by the disappearance of the acetal resonance and the appearance of a triplet at 3.61 ppm in the ^1H NMR spectrum. The ^1H NMR and ^{13}C $\{^1H\}$ NMR spectra of **3a** showed resonances consistent with the presence of the α-bromoester, such as the α-proton resonance at 4.34 ppm and the α-carbon resonance at 40.2 ppm. The ^1H NMR and ^{13}C $\{^1H\}$ NMR spectra of **3b** showed resonances consistent with the presence of the α-bromoester, such as the ester proton resonance at 4.16 ppm and the α-carbon resonance at 56.0 ppm. These resonances are sharp and clearly observed because these groups are far removed from the nanocluster surface and therefore the motion and spin relaxations should be similar to species freely rotating in solution. Additionally, resonances consistent with the butyl group were identified by a methyl proton resonance at 0.88 ppm and the methyl carbon resonance at 13.7 ppm in all nanocluster spectra. The region from 0.8 to 1.8 ppm in the ^1H NMR spectrum of germanium nanoclusters **1**−**3** is broadened (Figure 2). This is likely because some of these protons are on carbons close to the nanocluster core and these protons experience different chemical environments and perhaps restricted conformations. Additionally, in the ^{13}C-$\{^1H\}$ NMR spectra, multiple resonances are observed in the region assigned to carbons attached to germanium (∼32−33 ppm). These chemical shift assignments were based on ^{13}C $\{^1H\}$ NMR chemical shift of carbon atoms bonded to germanium where the germanium is bonded to another electropositive element, [55,56] the solution and MAS $^{13}C\{^1H\}$NMR spectrum of butyl-terminated nanoclusters, and the appearance of these multiple resonances in every $^{13}C\{^1H\}$ NMR spectra of nanoclusters **1**−**3**. To establish that these multiple peaks would not be seen in a molecular species, germanium tetrachloride was reacted with (6-tetrahydropyranyloxy)hexyl magnesium bromide followed by reaction with butyl lithium. The ^1H and $^{13}C\{^1H\}$ NMR spectra consisted of sharp resonances in all regions of the spectrum.

HRTEM Images of Nanoclusters 1 and 2. Samples of nanoclusters **1** and **2** were dissolved and sonicated in chloroform and were placed on holey carbon-coated 300-mesh electron microscope grids and then heated in a 120 °C oven overnight. Figure 4 shows a micrograph of nanoclusters **1** and the inset shows the lattice fringes consistent with the {220} germanium crystal plane. The average nanocluster size was calculated to be 3.7 ± 1.9 nm for 109 particles; however, particles as small as 1 nm and as large as 15 nm were observed. The average size is expected to be an overestimation since the smallest nanoclusters (1−2 nm) are difficult to discern because of the background of amorphous carbon from the grid. The presence of germanium is further confirmed by EDX. Figure 5 shows a micrograph of nanoclusters **2**; they are similar in size and shape with those shown in Figure 4, **1**, as expected.

(55) Jutzi, P.; Leue, C. *Organometallics* **1994**, *13*, 2898.
(56) Sekiguchi, A.; Yamazaki, H.; Kabuto, C.; Sakurai, H. *J. Am. Chem. Soc.* **1995**, *117*, 8025.

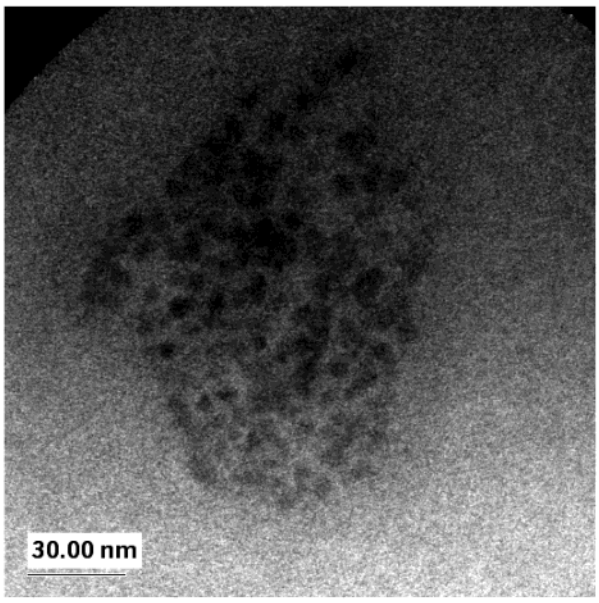

Figure 5. HRTEM image of nanoclusters **2**.

Grafting of Polymers. Polymer nanocomposites have been prepared of CdSe[57,58] and erbium doped Si[59] in poly(phenylene vinylene) and photoluminescence and electroluminescence have been observed. However, because the attachment of the nanocluster to the polymer is based on intermolecular forces of attraction rather than covalent bonds, dissolving or melting the sample causes loss of the integrity of the material. Polymer nanocomposites of erbium-doped silicon nanocrystals have also been prepared in poly(phenylene vinylene). In contrast, Farmer and Patten[60] have prepared hybrid nanostructures where a covalent linkage exists between polymethacrylate esters and a silica-coated CdS nanocluster. These materials can be dissolved and recast while maintaining the same disperse morphology.

*Polymerization of Styrene from the Nanocluster Surface To Yield a Hybrid Nanostructure (**4a**).* Further elaboration of the surface functionality of the nanoparticles was possible via polymerization initiated from the surface. The nanoclusters **3a** were heated at 110 °C with styrene, 4,4′-di(5-nonyl)-2,2′-bipyridine (dNbipy), copper(I) bromide, and xylene as an internal standard. The reaction rate appeared first order at low conversions but slowed as conversion levels above 40% were obtained (Figure 6). The molecular weights and molecular weight distributions of the grafted polymer chains were obtained by transesterification, by refluxing the composite materials in methanolic KOH and toluene for 16 h (Figure 7). The molecular weight of the grafted polymer increased with conversion and the molecular weight distributions were quite low ($M_w/M_n \leq 1.06$). The size distributions of the polymer-grafted nanoparticles as determined from GPC chromatograms (Figure 7) were higher than those of the grafted polymer, a result consistent with possibly both a size distribution of the nanoparticle cores and interparticle coupling during the

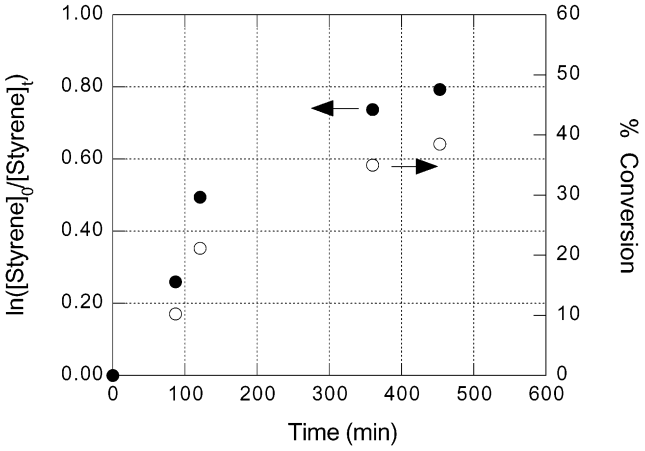

Figure 6. Kinetic plot for the polymerization of styrene using the surface α-bromoester-containing germanium nanocluster (ligand = dNbipy).

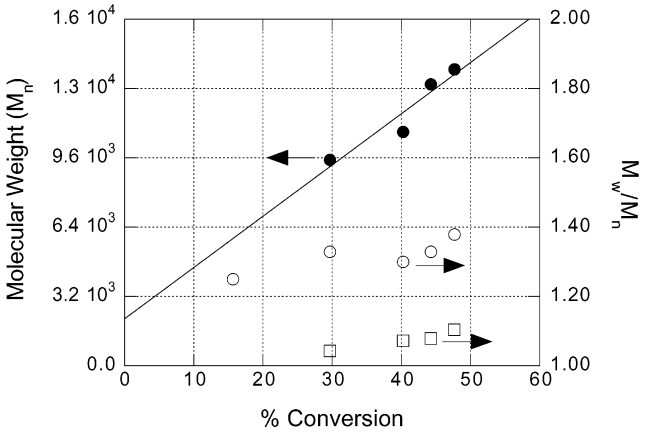

Figure 7. Plots of molecular weight and molecular weight distribution (for the hybrid nanocluster, ○, and for the degrafted polymer chains, ●, □ versus conversion for the polymerization of styrene using the surface α-bromoester-containing germanium nanocluster (ligand = dNbipy).

polymerization reaction. These results supported the conclusion that the grafting of the polystyrene from the nanocluster displayed the characteristics of a controlled/living radical polymerization.

*Polymerization of Methyl Methacrylate from the Nanocluster Surface To Yield a Hybrid Nanostructure (**4b**).* The nanoclusters **3b** were heated at 100 °C with methyl methacrylate, bis(triphenylphosphine)nickel(II) dibromide, and xylene as an internal standard. The reaction rate appeared first order up to 40% conversion. The composite nanocluster **4b** was highly soluble in chloroform and THF. Transparent films could be prepared on glass slides into a transparent film by slow evaporation from concentrated solutions of chloroform.

Photoluminescence of Functionalized Nanoclusters 1, 2, 3b, and 4b. Interest in semiconductor nanoclusters stems largely from the luminescent properties of these nanoclusters. If the nanoclusters are well-terminated, the photophysics of nanoclusters should be maintained regardless of solvent or variations in termination groups. The UV−vis spectra for nanoclusters **1**−**4b** in chloroform are similar, and the greatest absorbance occurs below 320 nm. This suggests that the

(57) Mattoussi, H.; Radzilowski, L. H.; Dabbousi, B. O.; Thomas, E. L.; Bawendi, M. G.; Rubner, M. F. *J. Appl. Phys.* **1998**, *83*, 7965.
(58) Schlamp, M. C.; Peng, X.; Alivisatos, A. P. *J. Appl. Phys.* **1997**, *82*, 5837.
(59) Ji, J.; Coffer, J. L. *J. Phys. Chem. B* **2002**, *106*, 3860.
(60) Farmer, S. C.; Patten, T. E. *Chem. Mater.* **2001**, *13*, 392.

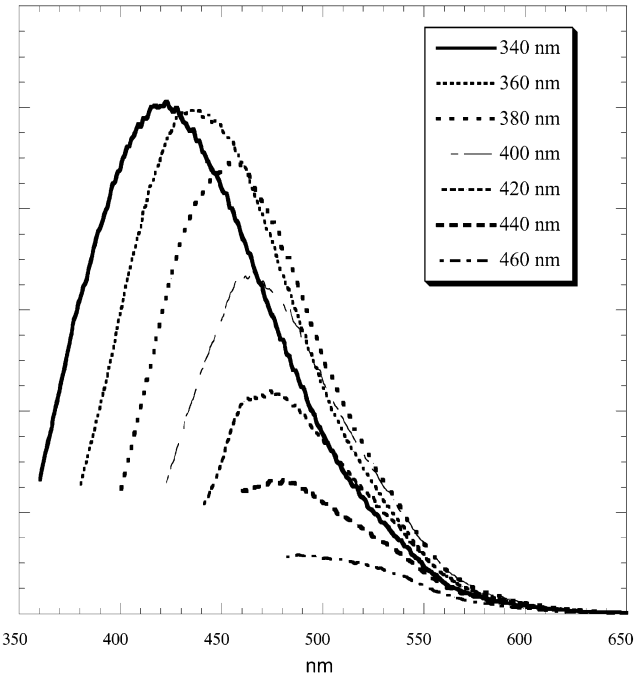

Figure 8. Normalized PL spectra for germanium nanoclusters-**1** (acetal-containing surface termination): PL for excitation 340−440 nm at 20-nm intervals with a 5-nm slit width.

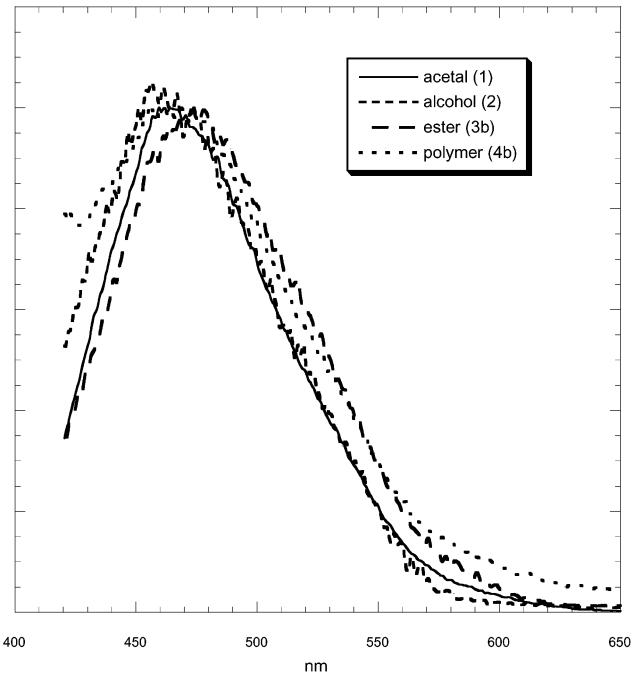

Figure 9. Normalized PL spectra at 400-nm excitation for germanium nanoclusters, -**1** solid line (acetal-containing surface termination), -**2** dashed line (alcohol- containing surface termination), -**3b** dotted line (ester-containing surface terminated), and -**4b** smaller dashed line (pMMA-containing surface termination). All spectra were recorded with a slit width of 5 nm.

nanoclusters that dominate the spectra are small, <4 nm.[28] These very small nanoclusters are difficult to discern in HRTEM, which provides evidence that our size distribution based on HRTEM images is biased toward the larger sizes. Figure 8 shows the PL spectra of nanoclusters **1** in spectrophotometric-grade chloroform and is similar to what has been observed in other alkyl-terminated nanoclusters.[34,36−38] Germanium nanoclusters produced by the described synthesis produce a continuous size distribution of nanoclusters, giving rise to the broadened PL spectra. However, the observed photoluminescence is dominated by the small nanoclusters, sizes smaller than 4 nm.[28] In addition, a monotonic shift with excitation wavelength is observed in the PL spectra, which is consistent with quantum confinement.[34] Figure 9 shows the PL for germanium nanoclusters of the same average size, prepared with four different termination groups, **1**, **2**, **3b**, and **4b**. The PL spectra are similar, as would be expected if the nanoclusters are well-terminated and the fluorescence is due to the germanium core. The fluorescence quantum efficiency for nanoclusters **2** in $CHCl_3$ in air was determined to be 1.5%. This number is similar in magnitude to reported quantum efficiencies of 0.5% for 4-nm germanium nanocrystals in a SiO_2 matrix.[61]

Conclusion

Germanium nanoclusters were prepared with termination groups containing functionality, and the functionality was readily manipulated to form other functionalized nanoclusters. It was demonstrated that ATRP could be used to prepare hybrid nanostructures of the germanium nanoparticles. NMR spectra, HRTEM images, and GPC data are consistent with modification on the nanocluster surface. Furthermore, changes at the termination group in nanoclusters did not alter their photophysics relative to the original nanoclusters **1**, which is consistent with a stable, well-terminated nanoparticle surface.

Acknowledgment. We thank Brian L. Phillips for obtaining the solid-state NMR data. Funding for R.S.T. was provided by the NSF Summer Program in Solid State Chemistry (2000) and a Petroleum Research Foundation Summer Faculty Fellowship administered by the ACS for Summer 2001 and 2002. This work was also supported by the NSF CAREER program (DMR-9733786) to T.E.P., by a NSF grant (DMR-9803074, 0120990) to S.M.K., and NSF grant CHE-9808183. K.A.P. received support from an NSF IGERT "Nanomaterials in the Environment, Agriculture and Technology". Work at the National Center for Electron Microscopy (NCEM) was performed under the auspices of the Director, Office of Energy Research, Office of Basic Energy Science, Materials Science Division, U.S. Department of Energy under Contract DE-Ac-03-76XF00098. We thank a reviewer of the original draft of this paper for suggesting that we examine our NMR spectra more closely.

CM021778H

(61) Kanemitsu, Y.; Uto, H.; Masumoto, Y.; Maeda, Y. *Appl. Phys. Lett.* **1992**, *61*, 2187.